ORIGINAL ARTICLE

Low Activity Microstates During Sleep

Hiroyuki Miyawaki PhD[1,2], Yazan N. Billeh PhD[3], Kamran Diba PhD[1]

[1]Department of Psychology, Box 413, University of Wisconsin—Milwaukee, Milwaukee, WI; [2]Current address: Department of Physiology, Osaka City University Graduate School of Medicine, Osaka, Japan; [3]Computation and Neural Systems Program, California Institute of Technology, Pasadena, CA

Study Objectives: To better understand the distinct activity patterns of the brain during sleep, we observed and investigated periods of diminished oscillatory and population spiking activity lasting for seconds during non-rapid eye movement (non-REM) sleep, which we call "LOW" activity sleep.

Methods: We analyzed spiking and local field potential (LFP) activity of hippocampal CA1 region alongside neocortical electroencephalogram (EEG) and electromyogram (EMG) in 19 sessions from four male Long-Evans rats (260–360 g) during natural wake/sleep across the 24-hr cycle as well as data from other brain regions obtained from http://crcns.org.[1,2]

Results: LOW states lasted longer than OFF/DOWN states and were distinguished by a subset of "LOW-active" cells. LOW activity sleep was preceded and followed by increased sharp-wave ripple activity. We also observed decreased slow-wave activity and sleep spindles in the hippocampal LFP and neocortical EEG upon LOW onset, with a partial rebound immediately after LOW. LOW states demonstrated activity patterns consistent with sleep but frequently transitioned into microarousals and showed EMG and LFP differences from small-amplitude irregular activity during quiet waking. Their likelihood decreased within individual non-REM epochs yet increased over the course of sleep. By analyzing data from the entorhinal cortex of rats,[1] as well as the hippocampus, the medial prefrontal cortex, the postsubiculum, and the anterior thalamus of mice,[2] obtained from http://crcns.org, we confirmed that LOW states corresponded to markedly diminished activity simultaneously in all of these regions.

Conclusions: We propose that LOW states are an important microstate within non-REM sleep that provide respite from high-activity sleep and may serve a restorative function.

Keywords: Slow wave sleep, EEG spectral analysis, microarousals, infraslow, SIA, NREM Sleep.

Statement of Significance

In large population neural recordings from sleeping rats, we observed long-lasting LOW activity epochs during which neuronal spiking and non-REM oscillatory activities were suppressed throughout the brain. LOW states were distinct from both DOWN/OFF states and microarousals. The likelihood of occurrence of LOW activity states varied inversely with sleep pressure, increasing with time asleep, particularly after REM, and decreasing following time awake. These LOW activity states may allow neurons to rest and repair and provide windows for potential transitions to waking.

INTRODUCTION

The brain passes through multiple distinct stages during sleep. Each stage produces distinct activity patterns, presumably playing important roles in the function of the brain. Non-rapid eye movement (non-REM) sleep, in particular, has been associated with sleep homeostasis, synaptic plasticity, memory consolidation, and a host of other sleep functions.[3–5] The signature activity pattern of non-REM sleep is the slow oscillation, an approximately 1-Hz alternation in cortical populations between UP states with robust ("ON") spiking activity and DOWN states where most neurons are silent or "OFF".[6] During UP/ON states, activity patterns can further display various faster oscillations, including sleep spindles (10–16 Hz) and hippocampal sharp-wave ripples (SWRs; 130–230 Hz).[7] On the other hand, DOWN/OFF states are characterized by the lack of any spiking activity lasting on the order of ~100 ms.[8]

A number of sleep functions have been attributed to the slower, longer lasting microstates of the brain. For example, the transition from the DOWN to the UP state during the slow oscillation can synchronize activity across the brain and provide a window for information transfer between the hippocampus and the neocortex.[5,9] Meanwhile, the transition to the DOWN state could induce synaptic long-term depression[4] in cortical networks. The DOWN state also provides neurons with respite from intensive discharge and ionic flux. It has been suggested that this respite allows for more efficient cellular restoration and maintenance.[10] Even longer lasting low- and high-activity phases have been reported during "infraslow" oscillations under anesthesia and waking.[11–15] The high-activity phases of these oscillations have been linked to "default mode" networks that subserve cognition,[11,13,16] while the low-activity phases reflect decreased blood flow and metabolic cost.[17]

Recently, we performed long duration recordings from the hippocampus and neocortex of freely moving and sleeping rats and report the prevalence of low-firing periods that lasted several seconds, far beyond the durations attributed to DOWN/OFF states. Following Pickenhain and Klingberg[18] and Bergmann et al.,[19] and because of their effects on neuronal firing, we call these "LOW" activity sleep states, but they have also been called "sleep small-amplitude irregular activity" (S-SIA).[20] We reserve the term SIA, as it was originally used, to describe quiet waking patterns.[21] We evaluate the occurrence of LOW activity sleep across the circadian cycle and describe its effects on other oscillatory activities within non-REM sleep, including slow-wave activity (SWA), sleep spindles, and SWRs, and on firing rates of neurons in the hippocampus and other brain regions. We contrast these with SIA states during quiet waking and microarousals (MAs) that are similar to LOW but display different electromyogram (EMG), local field potential (LFP), and electroencephalogram (EEG) patterns. We conjecture that LOW states provide neuronal rest within sleep and may prepare the brain for transitioning into quiet waking.

METHODS

We analyzed data from hippocampal region CA1 with neocortical EEG described in a previous study,[22] along with data from

CA1 and entorhinal cortex,[1] and from anterodorsal thalamus, and postsubiculum and medial prefrontal cortex,[2] freely available at http://crcns.org. Additional details of methods, including surgery, unit clustering, local field spectrum analysis, sleep state, spindle, and SWR detections, are provided in a previous paper[22] and summarized subsequently.

Animals, Surgery, and Data Collection

Four male Long-Evans rats (260–370 g; Charles River Laboratories, Wilmington, MA) were anesthetized with isoflurane and implanted with silicon microprobes in the dorsal hippocampus (2.00 mm lateral and 3.36 mm posterior from the bregma). In three of the rats, two stainless steel wires (AS 636; Cooner wire, Chatsworth, CA) were placed into the nuchal muscles to measure the EMG. Correlated high-frequency (300–600 Hz) signals from intracranial microprobe electrodes were used as an alternate measure of EMG[23,24] (iEMG) that does not depend on nuchal electrode placement. We took filtered signals from the top channel of each shank and calculated mean pairwise correlations among electrode pairs separated ≥400 µm in 500-ms bins. These two measures were independent but strongly correlated (r = 0.63 in 5-s time bins). In two of the rats, screws were inserted on the skull above the right frontal lobe (3.00 mm lateral and 2.50 mm anterior from the bregma) and attached to Nyleze insulated copper wires (overall diameter 0.13 mm; Alpha Wire, Elizabeth, NJ). The signals were recorded with a Digital Lynx recording system (Neuralynx, Bozeman, MT) and then processed using previously described methods.[25]

After a recovery period from surgery (>5 days), rats were placed on a water-restriction regimen to motivate track running and were given ad libitum water for 30 min each day. Three of four rats were maintained in a home cage except during the last 3 hr of dark cycles, during which they were put on an I-, L-, or U-shaped linear track in the same room and given water rewards on platforms after every traversal. A fourth rat was recorded only in the home cage during the light cycle. Two colored light-emitting diodes were mounted on the headstage, and the animals' movements were tracked with an overhead video camera. All procedures were in accordance with the National Institutes of Health guidelines and approved by the University of Wisconsin–Milwaukee Institutional Animal Care and Use Committee.

Unit Clustering and Cell Classification

Unit clustering and cell classification were performed as described previously.[25] We analyzed light cycles and dark cycles separately. For track-running sessions, we concatenated data from behavior on the track with the last 3 hr of the preceding dark cycle and the first 3 hr of the following light cycle. Putative pyramidal cells and interneurons were separated based on standard methods using spike waveforms, burstiness, refractory periods, and firing rates.[22,26–28] Units with an isolation distance <15 were considered potentially multiunits.[29]

Spectral Analyses

LFP, EMG, and EEG traces were low-pass filtered at 1250 or 1280 Hz using NDManager and its plugins[30](http://ndmanager.sourceforge.net). Power spectra were whitened and calculated using multitaper methods and the Chronux toolbox for Matlab[31] in 1-s windows.

Summary of Microstate Classification and Terminology

Non-REM sleep was separated into (i) LOW states (low EMG and low LFP), (ii) MAs (transient high EMG), and (iii) "non-REM packets" (low EMG) representing the remainder of non-REM sleep. Quiet waking and MAs were separated into SIA (low LFP) and non-SIA. REM was characterized by low EMG and high theta, while active waking featured high EMG and high theta. Further details are provided subsequently.

Microstate Detection

Sleep and waking were separated based on nuchal EMG and the animal's movement. In one rat which did not have nuchal EMG, we used iEMG instead. Data from this animal was consistent with the rest but was excluded from detailed EMG analyses in Figure 5B. Sleep was detected by low EMG power and no movement (defined below). The remainder was considered waking. EMG signals were first smoothed with a 1-s Gaussian filter and power was z-scored in 500-ms overlapping windows at 100-ms steps. A two-threshold "Schmitt" trigger was used to detect transitions between "low" and "high" EMG power at z scores = 0 and 0.5, respectively. Similarly, the thresholds for "no movement" and "movement" were set at 0.5 cm/s and 5 cm/s. Transient (<10 s) low EMG within waking was ignored. Transient high EMG power epochs (>0.1 s) within sleep were marked as MAs. Detected states underwent post hoc visual inspection and occasional manual modification. REM was inferred from high theta (described below) with no movement sandwiched between non-REM epochs. The theta (5–10 Hz) over (1–4 Hz plus 10–14 Hz) band ratio of the power spectral density was used to detect transitions between high theta and low theta, using custom-made MATLAB software written by Anton Sirota[27] based on the Hidden Markov Model Toolbox for Matlab (Kevin Murphy), followed by visual inspection. Sleep states with high theta were classified as REM and the remainder were classified as non-REM.[32,33] Similarly, waking periods with high theta were labeled "active awake" and the remainder were labeled "quiet waking." For the Peyrache et al.[2] data set, we used the provided non-REM, REM, and wakefulness timestamps, and considered only epochs >50 s.

LOW/SIA Activity Detection

LOW states were detected using the power spectra of the LFP in each brain region calculated in 1-s windows in sliding 0.1-s steps. The average power between 0.625–50 Hz was Gaussian filtered (σ = 0.5 s) and z-scored based on mean and *SD* within non-REM sleep. The resulting distribution could not be accounted for by a unimodal normal distribution ($p < 10^{-10}$; Shapiro-Wilk test; $p < 10^{-10}$ D'Agostino K^2 test). Rather, the two-dimensional (2D) histograms of filtered LFP power and mean firing rate during non-REM were consistent with two cluster clouds (Figure 1B). These cluster clouds, corresponding to LOW and non-LOW states, were similar when we used power spectra in different frequency bands (<20 Hz and 5–50 Hz) or window sizes (0.5 s and 2 s; Figure S4A). To evaluate goodness of cluster separation, the posterior probability of belonging to

the other state was calculated for each time bin using a Gaussian mixture model based on the mean, variance, covariance, and mixture weights of the two variables: LFP power and firing rate. Principal component analyses on LFP power spectra in log-spaced frequency bands (<100 Hz, z-scored within each band) also revealed first components (PC1) that featured a dominant contribution from lower frequencies (<10 Hz; Figure S1B) and produced similar segregation of detected states when plotted again low-frequency power (Figure S1C). Since the histogram of filtered power in itself showed two peaks (Figure 1B), to detect LOW states using LFP alone, we determined the position of the lower peak and the local minimum between the two peaks based on the second derivative of the smoothed (Gaussian filter, $\sigma = 0.1$ z-score) histogram. Periods in which z-scored power was lower than the local minimum were detected as candidate LOW states. If the LFP power in a candidate LOW did not drop below the lower peak of the histogram, it was discarded. Two consecutive LOW states separated by <0.5 s were concatenated. LOW states that even partially coincided with MAs were excluded from Figures 1–3 the analyses. We used these same thresholds to detect SIA during quiet waking and MA.

Finally, we also explored an alternative method to detect LOW states using hidden Markov models (HMM). Using the Viterbi algorithm, we separated non-REM epochs into two states independently using first low-frequency LFP power (<50 Hz) then mean firing rate in 1-s windows (sliding with 0.1-s steps). Bins consistent with LOW in both HMMs were labeled LOW. This method yielded similar LOW states as our main method (80.0% of LOW state bins were marked as LOW with HMM; Figure S4B) but appeared to be less conservative (50.6% of bins identified by HMM were not positive by the previous method); therefore, we opted for the simpler thresholding method described earlier.

For analyses in Figure 2, which required more accurate timestamps, onsets, and offsets were determined from population (MUA) firing rates. First, the mean firing rate in previously detected LOW and bordering non-LOW intervals were calculated. Then, a firing-rate threshold was determined for each LOW onset/offset. This threshold was set at the mean firing rate during LOW plus 20% of the difference in mean firing rate between LOW and its bordering non-LOW periods. Onset and offset timestamps were shifted accordingly.

SWR Detection

SWRs were detected following previously described methods.[34] First, the ripple band (130–230 Hz) power of the LFP was calculated during non-REM and quiet waking. Channels with the largest power in the ripple band were selected for each shank, and periods with power exceeding 1 *SD* of the mean in at least one of the selected channels were labeled as candidate events. Candidates with short gaps (<50 ms) were combined. Candidates shorter than 30 ms or longer than 450 ms were abandoned. Candidates were classified as SWRs if their peak power was >5 *SDs* of the mean.

Sleep Spindle Detection

Hippocampal LFP and neocortical EEG were band-pass filtered between 10 and 16 Hz (nearly identical results were observed with a wider 9–18 Hz band[22]). To detect hippocampal spindles, the LFP channel with the largest mean power during non-REM sleep was used. Candidate spindles in each signal were detected when amplitudes of the Hilbert transform exceeded 1.5 *SDs* above the mean for >350 ms.[35] Candidates were concatenated when inter-event intervals were <125 ms. Candidates with peak amplitudes below 4 *SDs* above the mean were abandoned. For each candidate, spindle troughs were detected. Candidates with intertrough intervals >125 ms (corresponding to slower than 8 Hz) were discarded.

Slow-Wave Activity

SWA was measured as power in the delta frequency band (0.5–4 Hz). To average across sessions, SWA was normalized to the session mean during non-REM sleep.

OFF/OFF' State Detection

Hippocampal OFF states arise from neocortical influence during SWA.[36–38] OFF states during non-REM were defined as periods with no CA1 units spiking for ≥50 ms.[8,39–41] ON states were defined as inter-OFF intervals in which ≥10 spikes were observed. To avoid spurious detection during sparse firing, only OFF states directly followed by ON states were included in the analyses[8] (note that this was not required for OFF' states). Average OFF state modulation of LFP (Figure 2D) was determined using the z-scored LFP.

To test whether LOW states might be equivalent to long-lasting OFF states under relaxed assumptions, we detected low-firing periods (OFF' states) by thresholding Gaussian-filtered ($\sigma = 100$ ms) multiunit activity (MUA) in 50-ms bins within non-REM sleep.[42] The threshold for each session was set at the value for which we obtained the same median MUA in OFF' and LOW states.

Modulation/Change Indices

Modulation index (*MI*) for variable X was defined as $(X_{LOW}–X_{non\text{-}REM\ packets}) / (X_{LOW} + X_{non\text{-}REM\ packets})$ for LOW and $(X_{SIA}–X_{non\text{-}SIA}) / (X_{SIA} + X_{non\text{-}SIA})$ for SIA. The change index (CI) for X was defined by $(X_{post}–X_{pre})/(X_{post} + X_{pre})$.

LOW/OFF' Modulation of Cells

Spikes were counted in 100-ms bins, and then means within LOW and OFF' states were calculated. The same number of bins were then randomly selected from outside LOW, to calculate surrogate means. This procedure was iterated 2000 times within each session separately. If the mean within LOW/OFF' was higher (or lower) than the top (or bottom) 0.5% of the shuffled data, the cell was marked as "activate" (or "suppressed"). We obtained qualitatively similar results with a novel community detection method.[43]

RESULTS

We performed spike detection and unit isolation of CA1 neurons on multiple sessions from both light and dark cycles in four animals. We first separated sleep and waking (including transient MAs) based on two measures of the electromyogram (EMG; see Methods for details) and movement and then separated sleep into REM (rapid eye movement) and non-REM, based on the presence of theta in the hippocampal LFP[32,33] (Figure S1A).

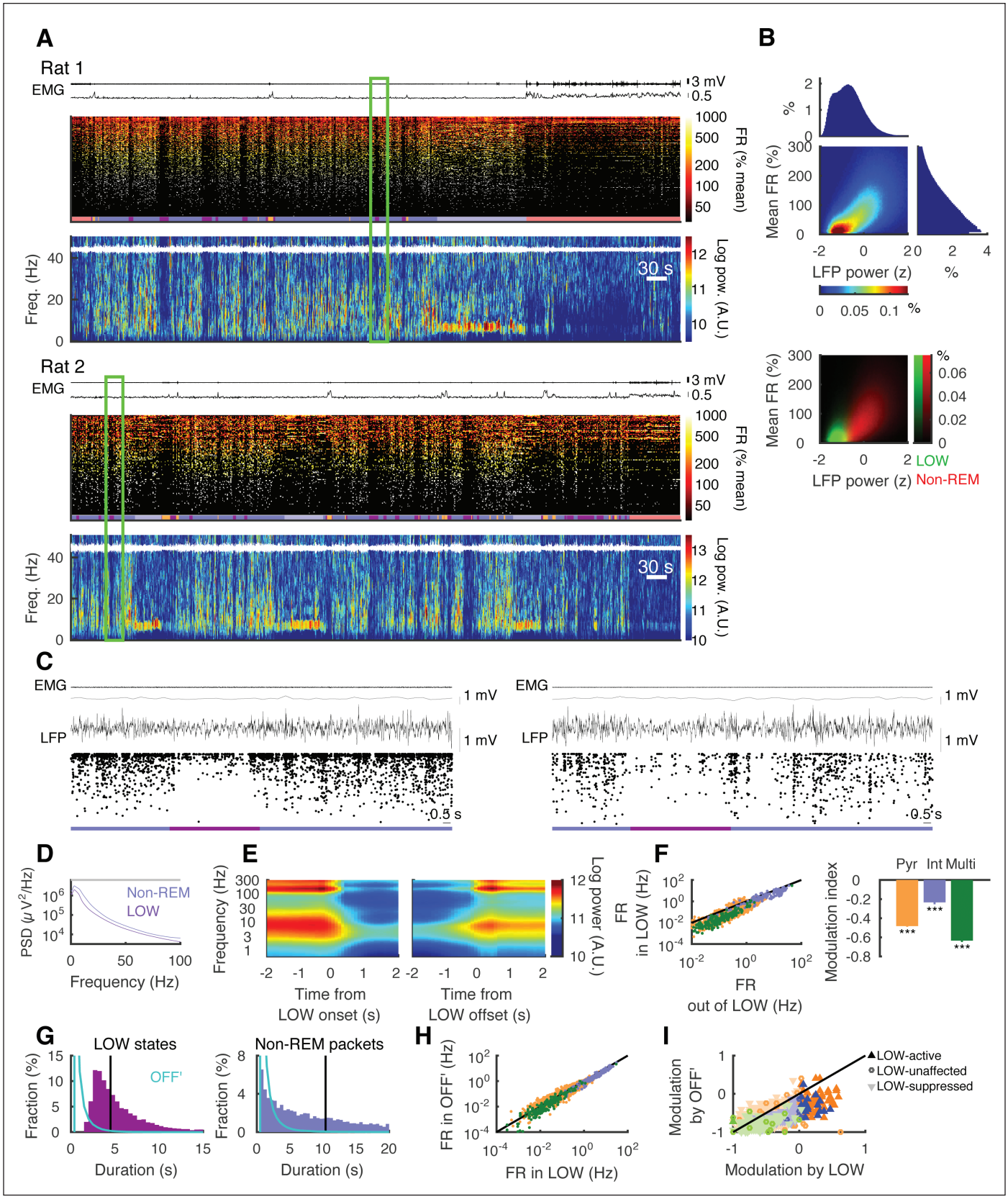
A
Rat 1
EMG
3 mV
0.5
1000
500
200
100
50
FR (% mean)
Freq. (Hz)
40
20
0
30 s
12
11
10
Log pow. (A.U.)
Rat 2
EMG
3 mV
0.5
1000
500
200
100
50
FR (% mean)
Freq. (Hz)
40
20
0
30 s
13
12
11
10
Log pow. (A.U.)
B
%
2
1
0
Mean FR (%)
300
200
100
0
-2
0
2
2
4
LFP power (z)
%
0
0.05
0.1
%
Mean FR (%)
300
200
100
0
%
0.06
0.04
0.02
0
-2
0
2 LOW
LFP power (z) Non-REM
C
EMG
1 mV
LFP
1 mV
0.5 s
EMG
1 mV
LFP
1 mV
0.5 s
D
PSD (μV²/Hz)
10⁶
10⁵
10⁴
Non-REM
LOW
0
50
100
Frequency (Hz)
E
Frequency (Hz)
300
100
30
10
3
1
-2
-1
0
1
2
-2
-1
0
1
2
Time from
LOW onset (s)
Time from
LOW offset (s)
12
11
10
Log power (A.U.)
F
FR
in LOW (Hz)
10²
10⁰
10⁻²
10⁻⁴
10⁻²
10⁰
10²
FR
out of LOW (Hz)
Modulation index
Pyr
Int
Multi
0
-0.2
-0.4
-0.6
-0.8
***
***
***
G
LOW states
OFF'
Fraction (%)
15
10
5
0
0
5
10
15
Duration (s)
Non-REM packets
Fraction (%)
8
4
0
0
5
10
15
20
Duration (s)
H
FR in OFF' (Hz)
10²
10⁰
10⁻²
10⁻⁴
10⁻⁴
10⁻²
10⁰
10²
FR in LOW (Hz)
I
Modulation
by OFF'
1
0
-1
-1
0
1
Modulation by LOW
LOW-active
LOW-unaffected
LOW-suppressed

In spike rasters from non-REM sleep, we observed striking and sporadic epochs of diminished activity lasting several seconds (Figure 1A-C; additional examples in Figure S2). These epochs, which we refer to as "LOW" states, were accompanied by strongly diminished power in the LFP (Figure 1D; $p < 10^{-10}$ for frequencies <100 Hz, Mann–Whitney *U* test [MWUT] with Bonferroni correction). To detect these low-activity epochs independent of firing rates, we calculated and set thresholds on the LFP power spectrum <50 Hz (Figure 1B-E; see Methods and Figures S3 & S4). 2D histograms of this low-passed LFP power and the mean firing rate in 1-s windows (sliding with 0.1-s steps) showed two cluster clouds within non-REM (but not REM; Figure S4D), reflecting distinct LOW and non-LOW sleep states (Figure 1B; individual animals shown in Figure S3A). Per a Gaussian mixture model, the median posterior probability of each assigned bin belonging to the other state was = 0.062.

We calculated a *MI* for each cell comparing firing rate between LOW states (n = 8151) and non-REM packets (n = 7973 defined as non-REM sleep excluding LOW states or MAs; see Methods). The distribution of *MI* was heterogeneous (Figure 1F, I), with a small subset of cells showing significantly positive *MI*. But overall, the mean *MI* was significantly < 0 for pyramidal cells ($MI = -0.48 \pm 0.01$, $p < 10^{-10}$, Wilcoxon signed-rank test [WSRT]), multiunits ($MI = -0.63 \pm 0.01$, $p < 10^{-10}$, WSRT) and interneurons ($MI = -0.23 \pm 0.02$, $p < 10^{-10}$, WSRT), indicating that the balance of excitation to inhibition is shifted toward relatively higher inhibition during LOW states.

In these recordings, we observed right-skewed distributions for the durations of LOW states (median = 4.5 s, range: 1.5–74.2s) and their interevent intervals (median = 10.4 s; Figure 1F). The 1-s windows we used for spectral calculations put a lower limit on the duration of detectable LOW states. Nevertheless, the mode of the histogram was at 2.75 s. The distributions of these variables were also right-skewed for OFF states detected using standard methods[8,40] but had shorter durations (median = 0.073 s, range: 0.050–2.641 s) and interevent intervals (median = 0.373 s). No secondary peaks were observed in any of the histograms, indicating the absence of oscillatory cycles. On average 11.7% of LOW (n = 19 sessions) consisted of OFF states. However, OFF states rarely lasted >2s (3 out of 585,388 detected OFFs). An alternate method for OFF state detection[42] yielded similar results (median duration = 0.070s; range: 0.010–4.900 s; see also Ji and Wilson's[42]; Supplementary Figure 12D), with only 51 OFF states >2s (out of 547,733 detected OFF states).

To further examine whether LOW states may be long-lasting OFF states, we iteratively relaxed the threshold of OFF to yield low-firing OFF' states (Figure 1G) with the median firing rates equal to LOW states; 74.0% (n = 19 sessions) of LOW qualified as OFF' states, but 65.0% of detected OFF' occurred outside LOW. Further, 36.8% of LOW states were in long OFF' (> 2s) while 34.4% of long OFF' was outside LOW. Thus, LOW and OFF' states overlapped but were not identical. As expected, virtually all (Figure 1H, 98.6%: 1578 pyramidal cells, 137 interneurons, and 208 multiunit clusters) were significantly suppressed during OFF' states, and few were significantly activated [/unchanged] (0.82% [/0.56%]: 14 [/7] pyramidal cells, 1 [/0] interneuron, and 1 [/4] multiunit clusters). But while most cells also fired significantly less during LOW states ("LOW-suppressed":90.1%, 1,451 pyramidal cells, 112 interneurons, and 194 multiunit clusters), a subset of cells were unchanged ("LOW-unaffected":5.4%, 81 pyramidal cells, 7 interneurons, and 17 multiunit clusters) or active specifically during LOW states ("LOW-active": 4.5%, 67 pyramidal cells, 19 interneurons, and 2 multiunit clusters). These proportions were significantly different from those of OFF' states ($p < 10^{-10}$ [/$p = 3.8 \times 10^{-7}$ /$p = 3.3 \times 10^{-3}$] for pyramidal cells [/interneurons/multiunit clusters], Pearson's chi-squared test; see also Figure 2C). Previous work indicates that these hippocampal "LOW-active" cells have place fields within an animal's sleep environment.[20,44,45] Consistent with a recent report,[45] these neurons showed a lower firing increase during SWRs than other cells ($p = 2.2 \times 10^{-1}$ and 1.3×10^{-3}, Tukey-Kramer test). Additionally, interneurons in general were more active during LOW than during OFF' ($p < 10^{-10}$, WSRT; see also Figure 2C). Overall, these observations demonstrate that LOW and OFF/DOWN states co-occur but remain distinct.

Figure 1—LOW activity microstates during non-rapid eye movement (non-REM) sleep. (A) Representative recordings from hippocampal region CA1. Top panels show the electromyogram (EMG; top and bottom traces depict nuchal EMG and intracranial EMG [iEMG], respectively) and raster plots of firing rates in 1-s bins (179 [/108] pyramidal cells, 13 [/2] interneurons and 42 [/3] multiunit clusters for Rat 1 [/Rat 2], ordered by mean firing rate), color normalized to the session mean. Color band beneath raster shows detected brain states (pink = quiet waking, purple/dark blue = LOW/non-LOW states within non-REM, light blue = REM, brown = microarousals). Bottom panels show power spectrograms of hippocampal local field potential (LFP; trace in white). (B) Two-dimensional histograms of z-scored LFP power <50 Hz and mean firing rates in 1-s bins during non-REM pooled across sessions (top) show two cluster clouds, reflecting LOW and non-LOW states. Side histograms display marginal distributions for each corresponding variable. In the bottom panel, comparison of detected LOW (green) and non-REM (red) bins. For individual sessions, see Figure S3. (C) Zoomed examples of green boxes from panel A. (D) Absolute mean power spectra of hippocampal LFP in LOW states and non-REM packets. Data were pooled across all sessions. SEMs were too small to be seen. Frequencies with significant difference are indicated with gray band on top. (E) LOW state onset- and offset-triggered CA1 LFP power spectra (for LOWs > 2 s). (F) Firing rates of pyramidal cells (n = 1599, orange), interneurons (n = 138, blue), and multiunit clusters (n = 213, green) were significantly lower within LOW states than out of LOW during non-REM. Black line is identity. Right panel shows mean modulation indices (*MI*; SEM error bars). (G) Durations and interevent intervals of LOW and OFF' states. Vertical lines indicate median duration (4.5 s) and interevent intervals (10.4 s). Distributions for OFF' states (cyan) are superimposed (median of duration [/interevent intervals] = 450 [/400] ms). (H) Firing rates within LOW and OFF' states were similar by definition (colors as in panel F). (I) Comparison of *MI* of firing rates between LOW and OFF' states for "LOW-active," "LOW-suppressed," and "LOW-unaffected" cells (colors as in panel F, with faded shading for "LOW-suppressed" cells). ** p < .01, *** p < .001.

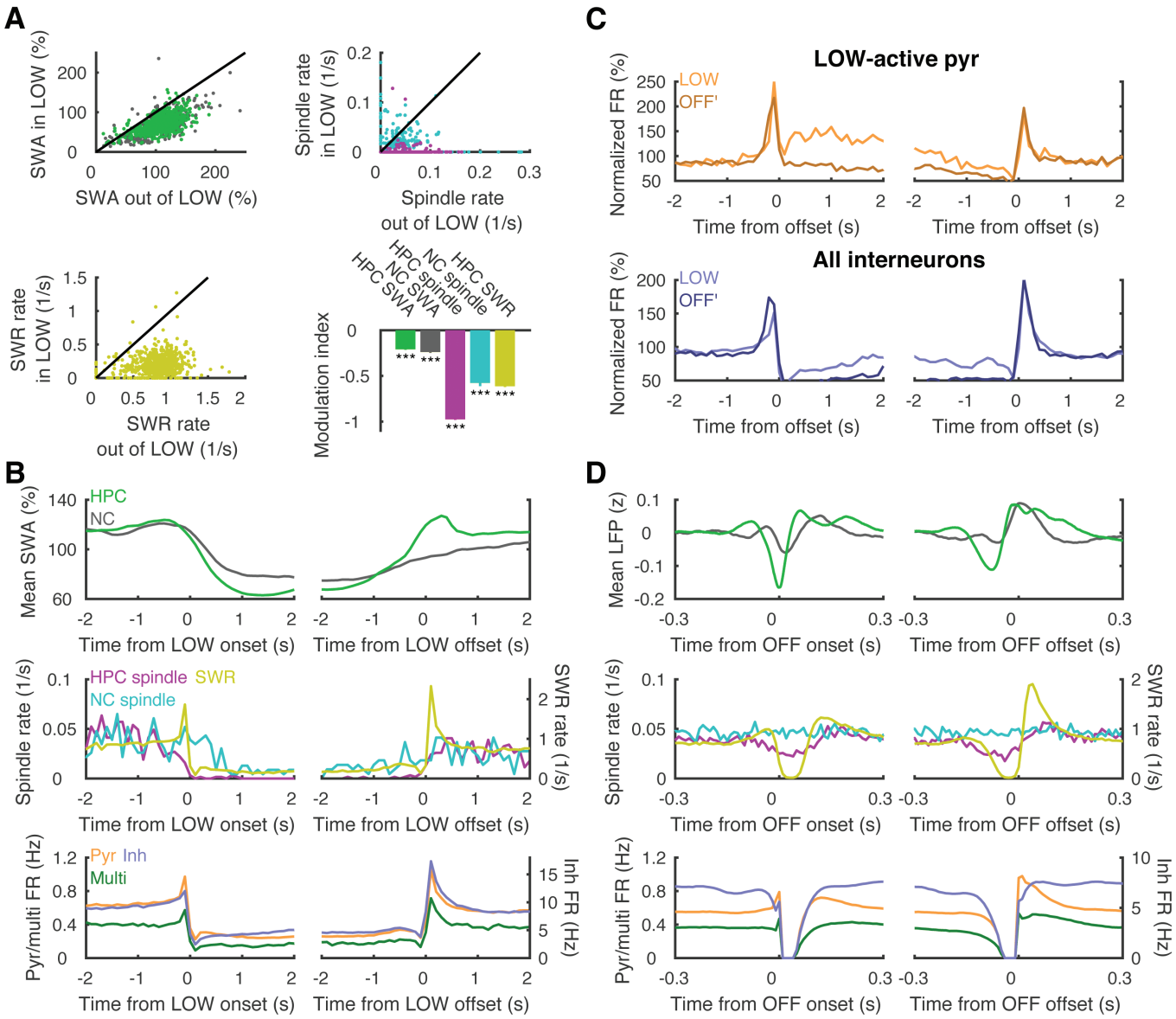

Figure 2—LOW state comodulation with hippocampal and thalamocortical oscillations. (A) Panels show mean slow-wave activity (SWA; power between 0.5 and 4 Hz) in hippocampus (HPC; green) local field potential (LFP) and neocortex (NC; gray) electroencephalogram (EEG), the incidence rates of HPC spindles (magenta), NC spindles (cyan), and HPC sharp-wave ripples (SWRs; yellow) for different non-rapid eye movement (non-REM) epochs (n = 927 for HPC and n = 436 for NC). Bottom-right panel shows modulation indices (*MIs*; SEM error bars). (B) Perievent triggered histograms of oscillatory events and neuronal firings after transitions to and out of LOW states (> 2 s). (B) SWA (top panel) in HPC (green; peak at 0.25 s) and NC (gray). Incidence rates of oscillatory events (middle panel) showing NC spindles (cyan), HPC spindles (purple), and SWRs (yellow). Mean firing rates (bottom panel) of pyramidal cells (orange, left axis), interneurons (blue, right axis), and multiunits (green, left axis). (C) Perievent triggered histograms of LOW-active pyramidal cells (top, n = 67) and all interneurons (bottom, n = 138) upon transitions to and out of LOW states and OFF' states (> 2 s). (D) Modulation of LFP (top), spindles. and SWRs incidence rates (middle) and neuronal firing (bottom) by OFF states. Note the shorter time scales compared to panel B. Error bars indicate standard error of the mean, *** p < .001.

Oscillatory and Spiking Activities Before and After LOW States

To examine how LOW sleep affects other oscillatory activities in non-REM, we detected SWA (mean power between 0.5–4 Hz), sleep spindles (10–16 Hz), and SWRs (130–230 Hz) in the CA1 region LFP and compared these before, during, and after LOW states (Figure 2A). Not surprisingly, SWA and the incidences of hippocampal spindles and SWRs were all significantly lower during LOW. To test for more global effects of LOW states, in eight sessions (from two animals), we also measured SWA and detected spindles on EEG above the neocortical frontal lobe. We observed lower SWA ($MI = -0.24 \pm 0.009$, $p < 10^{-10}$) and a lower incidence of sleep spindles ($MI = -0.53 \pm 0.05$, $p < 10^{-10}$) in the neocortical EEG during LOW sleep states (Figure 2B). We next compared activity 0.5–1.5 s after LOW offset to

0.5–1.5 s before LOW onset. While hippocampal SWA showed an immediate increase after transitioning out of LOW sleep (Figure 2B), SWA remained diminished in both the hippocampus ($\Delta M = -10.25 \pm 1.61\%$, $p < 10^{-10}$) and the neocortex ($\Delta M = -14.80 \pm 2.10\%$, $p = 1.0 \times 10^{-10}$). The incidence of spindles and SWRs also dropped and rose sharply at the onsets and offsets of LOW states, respectively. In particular, SWR incidence peaked 0.1 s before the transitions into and 0.1 s after transitions out of LOW (Figure 2B), indicating that SWRs tended to precede as well as follow LOW state transitions.[20] Similar to SWA, SWRs ($\Delta M = -0.165 \pm 0.02$ s^{-1}, $p = 1.7 \times 10^{-8}$), hippocampal spindles ($\Delta M = -0.020 \pm 0.004$ s^{-1}, $p = 7.0 \times 10^{-7}$), and neuronal firing rates (pyramidal cells $\Delta M = -0.070 \pm 0.008$ Hz, $p < 10^{-10}$, interneurons $\Delta M = -0.21 \pm 0.09$ Hz, $p = .007$, multiunit $\Delta M = -0.024 \pm 0.021$ Hz, $p = .006$) all remained lower for 0.5–1.5 s after LOW offset, except in LOW-active cells (Figure 2C) and did not return to pre-LOW levels until ~10s after LOW offset (not shown). In contrast, OFF states also elicited transient modulations but activities did not display lasting differences following OFF offset (Figure 2D), while OFF' states (>2s) provided distinctly different modulation from LOW states in LOW-active cells and interneurons (Figure 2C). Overall, these analyses demonstrate that neuronal activities transiently increase immediately before and after LOW but are strongly diminished during LOW and remain lower beyond its terminus.

LOW Sleep Across Cortical Regions

Based on the modulation of neocortical EEG activities by LOW states, and the neocortical origin of spindles and slow waves detected in the CA1 region,[36,37] we hypothesized that LOW states reflect a global decrease in activity throughout the cortex. To test this hypothesis directly, we analyzed two additional data sets from multiple brain regions obtained from http://crcns.org.[1,2] Applying the same detection methods to data from the entorhinal cortex (EC) and the hippocampus of rats recorded by Mizuseki et al.,[1] we confirmed the occurrence of LOW states in hippocampal region CA1 with coincident LOW states in layer 2/3 and layer 4/5 of the medial entorhinal cortex (Figure 3A and Figure S3B-E). For the second data set recorded by Peyrache et al.[2] in mice, we found simultaneous LOW states in the medial prefrontal cortex (mPFC), anterodorsal thalamic nucleus (ADn), postsubiculum (PoS), and hippocampus (Figure 3B and C). In both these data sets, the durations and interevent intervals of LOW states detected in the CA1 region were distributed similar to our own data set (Figure 3D).

Firing rates of neurons were significantly modulated in all brain regions considered (WSRT; Figure 3E): $MI = -0.40 \pm 0.008$ ($p < 10^{-10}$) in CA1, -0.10 ± 0.054 ($p = 3.8 \times 10^{-3}$) in EC L2/3, -0.23 ± 0.085 ($p = 3.7 \times 10^{-3}$) in EC L4/5, -0.17 ± 0.010 ($p < 10^{-10}$) in PoS, -0.10 ± 0.014 ($p = 1.1 \times 10^{-10}$) in mPFC, -0.04 ± 0.005 ($p < 10^{-10}$) in ADn. The strongest modulation was observed in CA1 and the weakest (but significant) modulation was seen in ADn ($p < 10^{-10}$, one-way analysis of variance [ANOVA]). The *MI* was significantly higher in CA1 compared to each of the other brain regions (Tukey-Kramer test, $p < .05$) except EC L4/5 and significantly lower in ADn than other regions except EC L4/5 and mPFC (Tukey-Kramer test, $p < .05$). In addition, the cross-correlogram between onsets/offsets of LOW states in CA1 and those in other regions showed a clear peak around zero (Figure 3F) with no secondary peaks. Auto-correlograms of LOW onsets/offsets (not shown) also showed no secondary peaks, again indicating that LOW was not reliably cyclic. To assess the temporal propagation of LOW between brain regions, we compared onset times within 1 s immediately before and after the CA1 LOW onset. Transition rates to LOW were higher in EC L2/3, EC L4/5, and PoS ($\Delta M = 0.049 \pm 0.017$ s^{-1}, $p = .004$ for EC L2/3, $\Delta M = 0.043 \pm 0.022$ s^{-1}, $p = .042$ for EC L4/5, $\Delta M = 0.159 \pm 0.019$ s^{-1}, $p < 10^{-10}$ for PoS) immediately after CA1 LOW onsets but were greater in mPFC preceding CA1 onset ($\Delta M = -0.040 \pm 0.012$ s^{-1}, $p = 7.6 \times 10^{-4}$) and unchanged in ADn ($\Delta M = 0.0004 \pm 0.056$ s^{-1}, $p = .95$ for ADn). These results indicate that LOW states are global and largely synchronous across brain regions, with a large fraction initiating earlier in prefrontal regions as also typically observed with slow waves.[46]

Likelihood of LOW Decreases Within Non-REM and Increases Across Sleep

We next examined when LOW states occur. In non-REM that followed REM sleep, LOW states were present throughout the epoch (Figure 4A) but decreased in likelihood of occurrence over epochs before REM ($p = 9.6 \times 10^{-10}$, one-way ANOVA followed by pairwise comparisons by Tukey-Kramer tests) and increased in likelihood over epochs that transitioned to waking ($p = 1.2 \times 10^{-3}$, one-way ANOVA followed by Tukey-Kramer tests). A similar pattern was also seen for MAs (Figure S5) but not for OFF states. And, while most (98.0%) LOW states did not terminate in waking, 62.1% of transitions from non-REM sleep to waking were transitions out of LOW sleep. Moreover, 48.2% of transient MA's were preceded by LOW (see below). Based on these patterns, we considered that LOW states may prepare the brain for a potential transition to waking. Consistent with this conjecture, we found a significant negative correlation between SWA (a well-established measure of sleep pressure[47]—here evaluated exclusively outside LOW) and the fraction of time in LOW ($r = -0.20$, $p = 2.4 \times 10^{-9}$; Figure 4B). Furthermore, we observed a lower likelihood of LOW following 3 hr of prolonged track running (6–9 a.m. each day; Figure 4C), when sleep pressure was highest,[22,47] this likelihood increased and plateaued following sleep.

Likewise, the fraction of time spent in LOW states (within non-REM) increased over sleep; comparing the first and last non-REM epochs within each extended sleep sequence (defined as sleep lasting >30 min without interruptions >60 s), the fraction of time in LOW significantly increased (change index [*CI*] = 0.17 ± 0.04, $p = 7.8 \times 10^{-5}$, WSRT; Figure 4D). Similarly, in non-REM/REM/non-REM triplets, the fraction of time in LOW was higher in the second non-REM ($CI = 0.11 \pm 0.02$, $p = 5.6 \times 10^{-9}$). These changes in the frequency of LOW accounted for a large fraction of the firing rate decreases across sequential non-REM sleep epochs ($R^2 = 0.42$, $p < 10^{-10}$). However, sleep-dependent firing rates decreased both outside and within LOW states and previously reported correlations between firing decreases, and spindles and SWRs[22] remained significant when LOW periods were excluded ($r = -0.30$ $p = 8.3 \times 10^{-8}$ and $r = -0.22$ $p = 1.0 \times 10^{-4}$

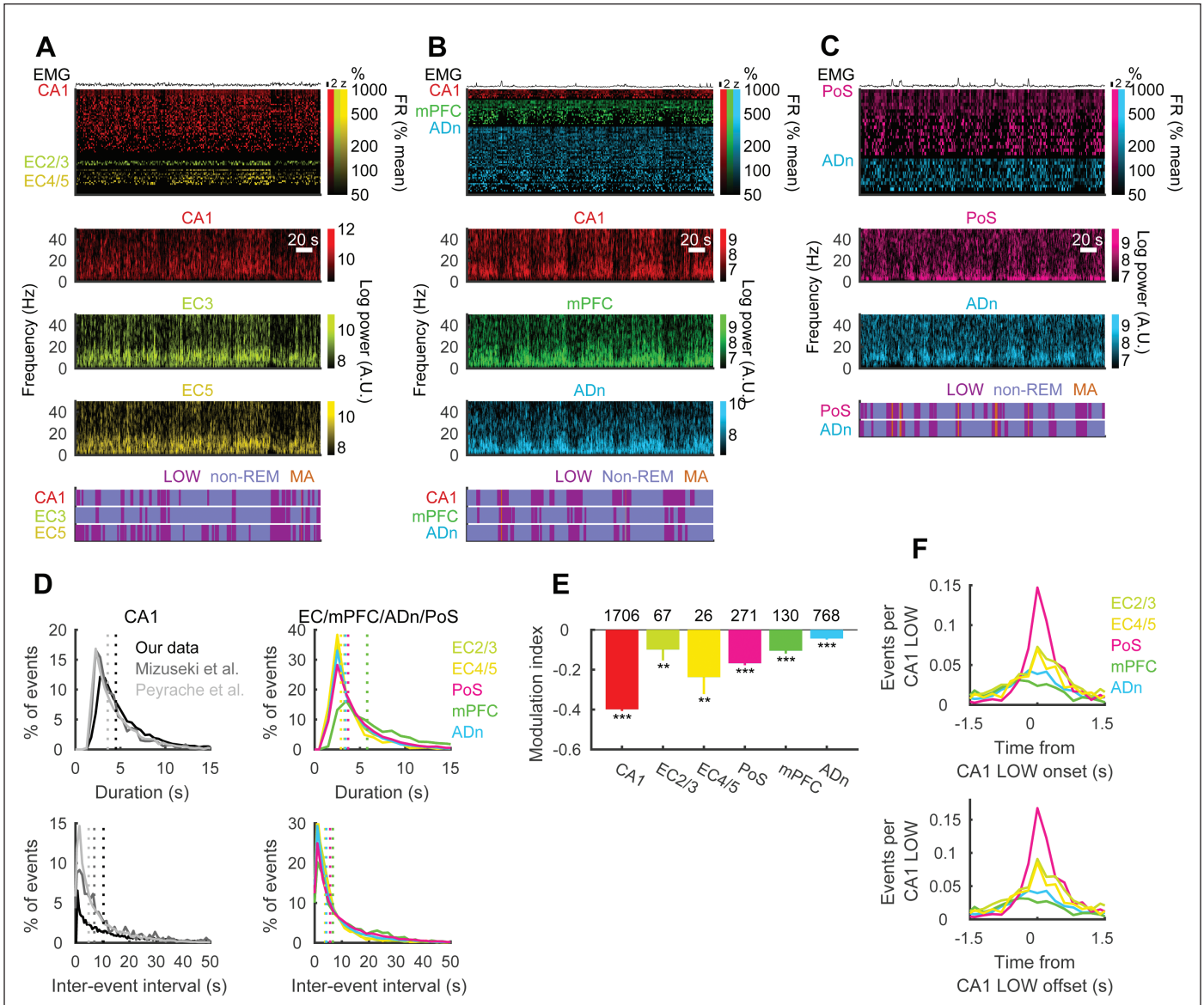

Figure 3—LOW states across different brain regions. (A–C) Examples of LOW states in data sets from rat[1] (A) and mouse[2] (B & C). Top panels show spike raster plots in 1-s bins. Color indicates brain regions, and brightness indicates firing rates normalized to the session means (46 CA1 cells, 6 entorhinal cortex [EC] L2/3 cells, and 15 EC L4/5 cells in A; 7 CA1 multiunits, 19 medial prefrontal cortex [mPFC] cells and 47 anterodorsal thalamic nucleus [ADn] cells in B; 21 postsubiculum [PoS] cells and 11 ADn cells in C). Intracranial electromyogram (iEMG) is shown on the top. Middle panels depict power spectra of simultaneously recorded local field potentials (LFPs). Bottom panels show frequently synchronous LOW states detected separately for these regions. (D) Durations and interevent intervals for LOW states in CA1 (left panels) and other brain regions (right panels) were distributed similarly across data sets and brain regions. Vertical lines indicate median values. (E) Firing rates were modulated by LOW states in all brain regions (*n* = numbers of cells, indicated above; standard error of the mean error bars). (F) Cross-correlograms between LOW states in CA1 and other brain regions show largely synchronous LOW state onsets and offsets. ** p < .01, *** p < .001.

for spindles and SWRs, respectively). In contrast to sleep, the fraction of time in LOW decreased following the 3-hr awake track-running sessions (Figure 4D; first hour post vs. last hour pre $CI = -0.23 \pm 0.07$, p = .047, WSRT). Following stable waking periods (lasting > 15 min without interruptions > 60 s), the fraction of time in the LOW state also decreased but not significantly (Figure 4D; $CI = -0.15 \pm 0.10$, p = .15). These results demonstrate that LOW states are more frequent with increasing sleep, after sleep pressure has dissipated, and decrease following wakefulness, as sleep pressure accumulates.

SIA States in Quiet Waking and MA

A review of the literature reveals that LOW sleep states share features with SIA and other low-activity states observed during quiet waking and MAs[11–15,20 21,24,48,49] (see also Figure S5). In the following (see Table 1), we separated non-REM sleep into (i) LOW states (low EMG and low LFP), (ii) MAs (transient high EMG), and (iii) "non-REM packets" (low EMG). Quiet waking and MAs were further separated into SIA (low LFP) and non-SIA periods. We detected MAs (median = 3.0 s; Figure 5A; see also Figure 1A) that interrupt non-REM sleep using EMG alone. LOW and MA

states displayed distinctly different EMG levels (Figure 5B), but frequently (48.2% of the time, n = 8980) MAs were preceded by LOW states and 39.8 % of MA's transitioned into LOW states. We supposed that longer lasting LOW states may eventually transition into MA; however, we instead found that pre-MA LOW states were typically shorter, lasting 2.5 s (median). Post-MA LOW states were also brief, lasting 1.4 s (median).

We then applied LOW detection to both MA and quiet waking periods in our recordings to see if similar activity patterns are also observed then. Following the earlier literature,[21,44,45,50] we use the term "SIA" to refer to periods with low LFP power < 50 Hz (similar to LOW) during waking and MA, when EMG is high; 44.5% ± 2.7 % (n = 19) of time in MA was thus classified as SIA (median MA-SIA duration = 2.9 s). Additionally, much of quiet waking similarly qualified as SIA (56.1 ± 3.4 %), compared to 21.9 ± 2.6 % of non-REM in LOW. Durations and interevent intervals of SIA states in quiet waking were distributed similar to sleep LOW,

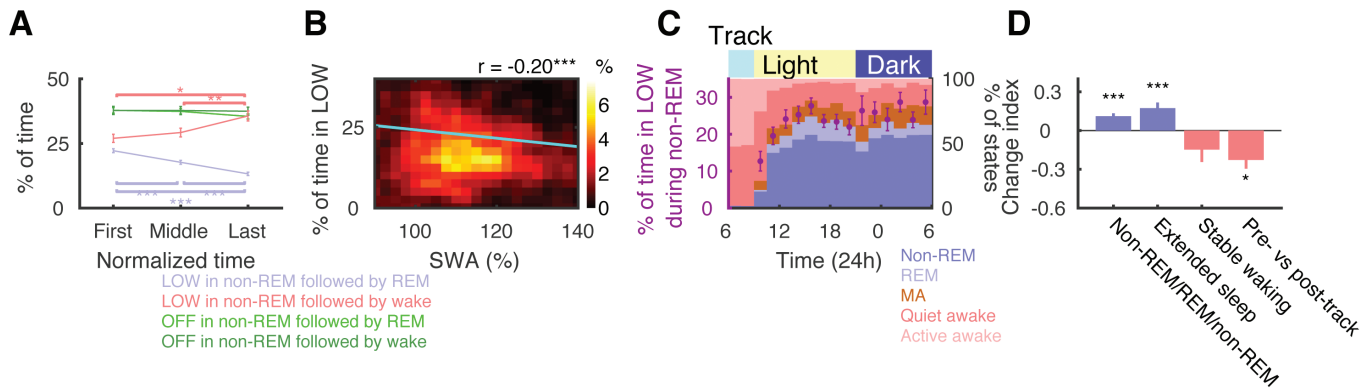

Figure 4—LOW states increased with decreasing sleep pressure. (A) The fraction of time in LOW within non-rapid eye movement (non-REM) epochs followed by REM (blue, n = 427 epochs) or followed by quiet waking (pink, n = 225 epochs), and the fraction of time in OFF states followed by REM (light green) or quiet waking (dark green). (B) Slow-wave activity (SWA), calculated exclusively outside LOW, was inversely correlated with the fraction of time in LOW states (n = 927 non-REM epochs). Regression line (cyan) is superimposed on density map of epoch means. (C) The fraction of time (within non-REM) in LOW states across the 24-hr cycle (with track running sessions from 6 to 9 a.m.). Background colors indicates percentage of time spent in each behavioral/sleep state. (D) Change indices for fraction of time in LOW between non-REM epochs interleaved by REM (n = 295), the first and last non-REM epochs in extended sleep (n = 90), non-REM epochs separated by stable waking (> 15 min; n = 35), and non-REM epochs immediately before and after 3-hr track sessions (n = 7). * p < .05, ** p < .01, *** p < .001, error bars indicate SEM.

Table 1—Activity during LOW, non-REM, and MA states[a].

	LOW	Non-REM Packets	MA
Duration (s)	4.5 ± 3.6	10.4 ± 20.6	3.0 ± 4.0
Nuchal EMG (z)	−0.204 ± 0.007	−0.213 ± 0.007	0.184 ± 0.009
iEMG (z)	−0.407 ± 0.010	−0.372 ± 0.011	1.00 ± 0.028
LFP power (A.U.)	37.0 ± 0.5	66.7 ± 1.1	47.2 ± 0.7
Hippocampal SWA (%)	69.3 ± 0.7	107.8 ± 0.9	72.2 ± 1.4
NC SWA (%)	64.7 ± 1.7	103.0 ± 2.1	50.7 ± 1.6
HPC spindle incidence (1/s)	0.0005 ± 0.0001	0.0479 ± 0.0030	0.0160 ± 0.0012
Neocortical spindle incidence (1/s)	0.019 ± 0.002	0.060 ± 0.005	0.027 ± 0.002
SWR incidence (1/s)	0.252 ± 0.005	0.801 ± 0.009	0.412 ± 0.010
FR of pyramidal cells (Hz)	0.292 ± 0.012	0.630 ± 0.018	0.450 ± 0.015
FR of interneurons (Hz)	5.24 ± 0.43	8.93 ± 0.70	7.48 ± 0.56
FR of multiunit clusters (Hz)	0.20 ± 0.14	0.41 ± 0.21	0.31 ± 0.20
FR of LOW-active pyr cells (Hz)	0.85 ± 0.08	0.55 ± 0.06	0.86 ± 0.10

[a]Mean ± SEM are provided for all variables except for duration (median ± interquartile range).

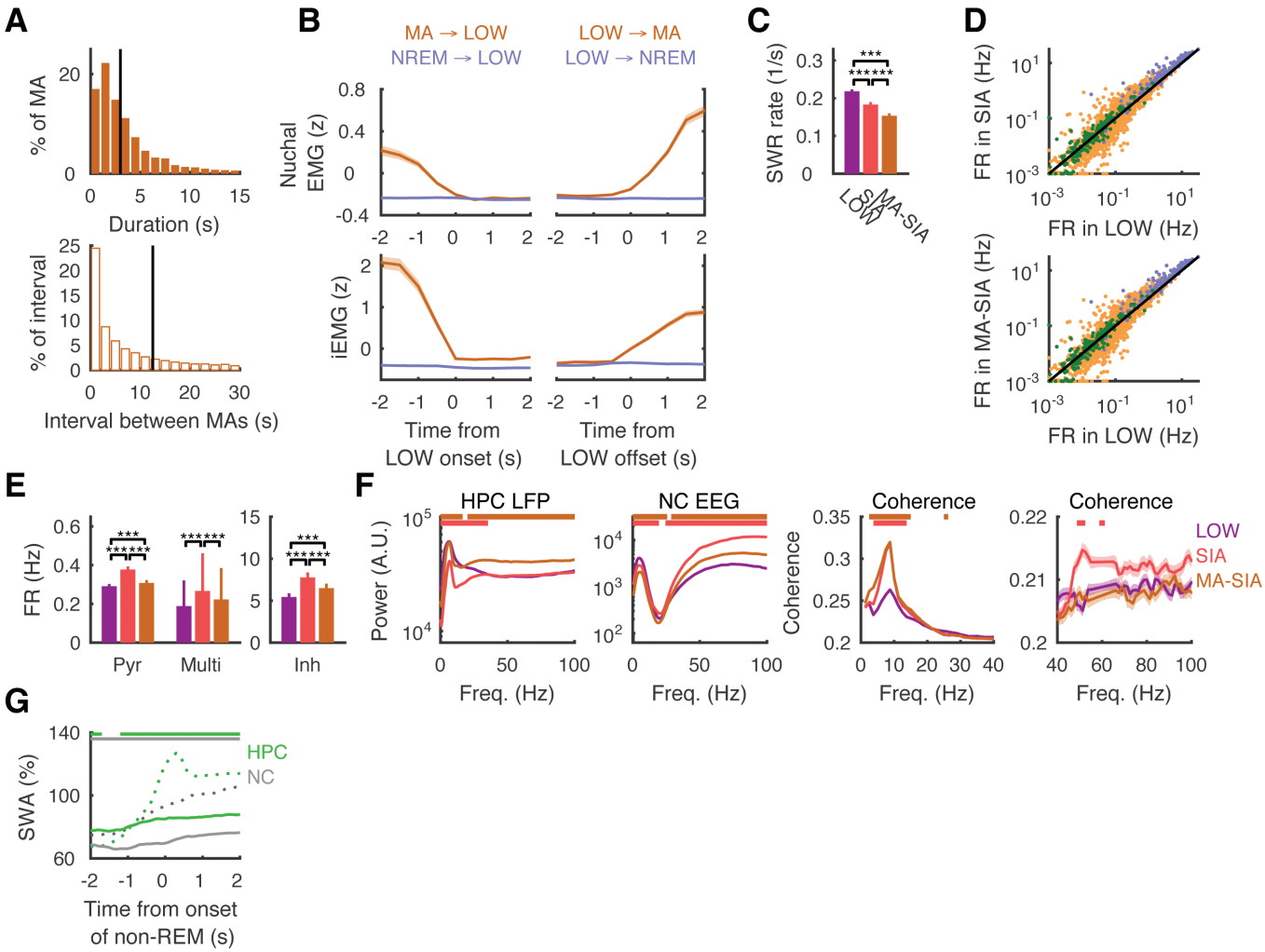

Figure 5—Comparison of LOW and small-amplitude irregular activity (SIA) states. (A) Durations of microarousals (MAs; top) and inter-MA intervals (bottom). Vertical lines indicate median values (3.0 s for MAs and 12.5 s for inter-MA intervals). (B) Electromyogram (EMG) amplitudes obtained from nuchal muscles (top) and derived from intracranial electrodes (bottom; see Methods) were aligned to transitions between LOW states (> 2 s) and non-REM packets (blue) and MAs (brown). (C) Comparison of incidence rates of SWRs in SIA, MA-SIA, and LOW sleep. (D) Mean firing rates of pyramidal cells (orange), interneurons (blue), and multiunits (green) were similar in LOW and SIA (black line shows the identity). Cells that did not fire during LOW and SIA/MA-SIA are plotted on x- and y-axes, respectively. (E) Mean firing rates of pyramidal cells and interneurons in SIA and MA-SIA compared to LOW. (F) Power spectra of hippocampal local field potential (LFP) and neocortical electroencephalogram (EEG; left panels) and coherence between these regions (right panels) with significant differences in theta and gamma frequency bands ($p < .001$). (G) Mean slow-wave activity (SWA; power 0.5–4 Hz) compared between transitions from MA and LOW to non-REM packets (dashed lines, see Figure 2C). Significant differences are indicated with color bands on top ($p < .05$). ** $p < .01$, *** $p < .001$, error bars indicate SEM and shading indicates 95% confident intervals.

although SIA states were slightly longer (median = 6.3 s, $p < 10^{-10}$, MWUT) with shorter interevent intervals (median = 4.1 s, $p < 10^{-10}$). Unexpectedly, SIA featured faster (but still small) head speed compared to other (non-SIA) quiet waking, suggestive of muscle twitches or grooming (M = 2.4 cm/s during SIA and M = 1.6 cm/s during quiet waking, $p < 10^{-10}$, WSRT), though substantially less than active waking (M = 4.6 cm/s, $p < 10^{-10}$, WSRT). Interestingly, a study in head-fixed mice, published after our initial submission, also found greater whisking, pupil diameter, and treadmill velocity during SIA,[48] further demonstrating that unlike LOW, SIA should not be considered a sleep state.

Next, we compared neuronal activity between LOW and SIA. Slow waves and spindles were not observed during waking or SIA but SWRs were. As expected,[20] SWR incidence rates were significantly modulated by SIA ($MI = -0.41 \pm 0.017$, $p < 10^{-10}$, WSRT) and by MA-SIA (-0.59 ± 0.014, $p < 10^{-10}$). SWR incidences in SIA and MA-SIA were lower than in non-REM LOW (Figure 5C). Firing rates of neurons were generally similar in LOW and SIA (Figure 5D). However, some units appeared to be active only during LOW, without firing in SIA (i.e. see 31 points along x-axis of Figure 5B). These cells had no reliable place fields within the home cage (in 29 out of 31 cases, peak place field firing was < 0.3 Hz). Nevertheless, overall firing rates were

slightly higher in SIA than LOW ($p < 10^{-10}$ for pyramidal cells, $p = 3.9 \times 10^{-6}$ for multiunit cluster, and $p < 10^{-10}$ for interneurons, WSRT; Figure 5E).

To further examine differences between LOW and SIA, we also compared the power spectra of the hippocampal LFP and neocortical EEG between MA-SIA, SIA, and LOW states (Figure 5F). While the same threshold was used to detect both LOW and SIA, overall patterns in SIA were quite different from LOW. Hippocampal LFP had significantly lower power <35.4 Hz in SIA states than in LOW ($p < .001$, MWUT with Bonferroni correction), consistent with less synchronization during waking states, and in the neocortical EEG spectrum, SIA had slightly lower power < 16.5 Hz and stronger power > 20.1 Hz ($p < .001$; Figure 5F). Moreover, hippocampal LFP and neocortical EEG demonstrated enhanced coherence ($p < .001$) near theta and gamma bands during SIA indicating a greater level of cortical activation and arousal during SIA, and in theta (but not gamma) during MA-SIA, perhaps indicative of drowsiness. Finally, SWA activity showed an immediate partial rebound following transition from LOW to non-REM (Figures 2F & 5G) but not from MA to non-REM ($p < .05$; MWUT with Bonferroni correction). Thus, LOW is a microstate *within* non-REM sleep, whereas MA is an *interruption* of sleep and resets the buildup of SWA.[47]

DISCUSSION

In summary, we observed long-lasting suppressed activity periods during non-REM sleep, which we call LOW activity sleep. In earlier studies in natural sleep, microstates were observed that share features with the LOW activity sleep states we describe (e.g. [18, 19, 51, 52]). However, population spiking activity was not available in those studies, and it could not be determined whether these low-amplitude epochs were desynchronized because of high or low neuronal firing activity. Jarosiewicz and colleagues[20,44] also studied SIA and LOW in large-scale hippocampal unit recordings and made similar observations about neuronal firing and SWRs. Our study provides a quantitative confirmation and extends on their reports in multiple ways.

LOW sleep was characterized by a strong decrease in population spiking and oscillatory activities including slow waves, sleep spindles, and SWRs (Table 1). While most activities rebounded, their levels remained diminished for several seconds, indicating a lingering effect of LOW states beyond their termini.[24,49] SWRs, however, were transiently increased immediately before and after LOW, potentially reflecting homeostatic rebound[53] and a vulnerability for epilepsy,[54,55] although we saw no evidence of pathology. We also showed that LOW states strongly suppress neuronal activity not just in the hippocampus but throughout the brain, including the entorhinal cortex, prefrontal cortex, postsubiculum, and anterodorsal thalamus. This suppressed activity lasted much longer than typical OFF states and was accompanied by increased firing in a LOW-active subset of neurons.[44,45] Interestingly, both OFF and LOW states were preceded by transient increased firing, suggesting a common onset mechanism, such as a hyperpolarizing current,[14,56] which may also be present during SIA.[48] But importantly, LOW states featured higher levels of interneuron firing than did OFF' states. Ultimately, intracellular recording is needed to test whether DOWN-level membrane potentials[6] are present during LOW and further examine commonalities and differences between LOW and DOWN/OFF states.

LOW sleep occurred not just after REM but throughout non-REM sleep and may be triggered in response to high neuronal activity, from either REM sleep or UP/ON states and SWRs,[8,22] that increase the need for neuronal rest and restoration. Vyazovskiy and Harris[10] recently proposed that a global quiescent state may be valuable for cellular repair and restoration of organelles. LOW states may be suitable for carrying out such functions. We uncovered an inverse relationship between the rate (fraction of time) of LOW sleep with sleep pressure, with low likelihood in early non-REM sleep following waking but increasing likelihood in late sleep. The neuronal activities that occur in non-REM outside LOW states (e.g. slow waves, spindles, and SWRs) have been linked to some of the memory benefits of sleep[4,5,7] and are more prevalent in early sleep.[22] These observations, combined with the greater fidelity of replay during early sleep,[57] may support the idea that early sleep serves for circuit modification, including synaptic downscaling,[4] while late sleep, under decreased sleep pressure, may support cellular restoration and upkeep.[10,58]

We demonstrated that LOW states are distinctly a sleep state, with lower EMG, lower gamma and gamma coherence, but higher low-frequency (delta and theta) activity, and greater SWA rebound than SIA or quiet waking. Unfortunately, some confusion may arise from inconsistent terminology in the literature. For example, LOW sleep states were called "S-SIA" by Jarosiewicz et al.,[20] but later "SIA" by the same authors[44,50] and more recently by Kay et al.[45] They also appear to share features with phase B of the cyclic alternating pattern in non-REM sleep.[49,52] We propose that SIA should be reserved for the waking state, as originally described by Vanderwolf[21] and later employed by others,[20,48] while LOW amplitude/LOW activity sleep is best reserved for the sleep state, as also originally used.[18,19] Nevertheless, it is feasible that collectively LOW sleep and waking SIA represent the sleep and waking extremes of a continuum of microarousals.[24,59] Consistent with this notion, we observed frequent transitions between LOW states and MA, and MAs demonstrated both SIA and non-SIA periods. SIA periods (relative to LOW) showed less slow activity, and higher gamma power and gamma coherence between hippocampal LFP and neocortical EEG, consistent with cortical activation, and hippocampal place-cells that encode the animal's sleep location fire during both LOW sleep and SIA[20,44,45] as if in preparation for spatial cognition.

LOW states also appear to share features with the low-activity phase of infraslow oscillations,[11–15] although we observed no evidence for repeated oscillatory cycles in LOW (Figure 1E). Recent evidence suggests the low-activity phases of infraslow oscillations are produced by long-lasting hyperpolarizing potassium currents, mediated by ATP-derived adenosine released from astrocytes.[14] Such nonsynaptic currents may produce LOW states, potentially accounting for the parallel firing decreases observed in both pyramidal cells and interneurons, as well as the lingering effect from LOW states on subsequent activity patterns (see also ref[24]). Interestingly, infraslow low-activity phases coincide with large-scale calcium waves in astrocytic networks,[60] which may account for their global nature. Cerebral blood flow during these low-activity phases

is ~10% lower, indicating that they are detectable in global BOLD activity as well as LFP.[16] Given these facts, along with the central role that astrocytes and adenosine play in cellular repair,[61] energy metabolism,[62] and mediating sleep pressure,[63] they may also play a central role in the genesis and function of LOW states.

REFERENCES

1. Mizuseki K, Diba K, Pastalkova E, Teeters J, Sirota A, Buzsáki G. Neurosharing: large-scale data sets (spike, LFP) recorded from the hippocampal-entorhinal system in behaving rats. F1000Res. 2014; 3: 98.
2. Peyrache A, Buzsáki G. Extracellular recordings from multi-site silicon probes in the anterior thalamus and subicular formation of freely moving mice. CRCNS.org; 2015. doi: 10.6080/K0G15XS1.
3. Rechtschaffen A. Current perspectives on the function of sleep. Perspect Biol Med. 1998; 41(3): 359–390.
4. Tononi G, Cirelli C. Sleep and the price of plasticity: from synaptic and cellular homeostasis to memory consolidation and integration. Neuron. 2014; 81(1): 12–34.
5. Rasch B, Born J. About sleep's role in memory. Physiol Rev. 2013; 93(2): 681–766.
6. Steriade M, Nuñez A, Amzica F. A novel slow (< 1 Hz) oscillation of neocortical neurons in vivo: depolarizing and hyperpolarizing components. J Neurosci. 1993; 13(8): 3252–3265.
7. Buzsaki G. Hippocampal sharp wave-ripple: A cognitive biomarker for episodic memory and planning. Hippocampus 2015;25:1073–188.
8. Vyazovskiy VV, Olcese U, Lazimy YM, et al. Cortical firing and sleep homeostasis. Neuron. 2009; 63(6): 865–878.
9. Sirota A, Buzsáki G. Interaction between neocortical and hippocampal networks via slow oscillations. Thalamus Relat Syst. 2005; 3(4): 245–259.
10. Vyazovskiy VV, Harris KD. Sleep and the single neuron: the role of global slow oscillations in individual cell rest. Nat Rev Neurosci. 2013; 14(6): 443–451.
11. Chan AW, Mohajerani MH, LeDue JM, Wang YT, Murphy TH. Mesoscale infraslow spontaneous membrane potential fluctuations recapitulate high-frequency activity cortical motifs. Nat Commun. 2015; 6: 7738.
12. Aladjalova NA. Infra-slow rhythmic oscillations of the steady potential of the cerebral cortex. Nature. 1957; 179(4567): 957–959.
13. Hiltunen T, Kantola J, Abou Elseoud A, et al. Infra-slow EEG fluctuations are correlated with resting-state network dynamics in fMRI. J Neurosci. 2014; 34(2): 356–362.
14. Lörincz ML, Geall F, Bao Y, Crunelli V, Hughes SW. ATP-dependent infra-slow (<0.1 Hz) oscillations in thalamic networks. PLoS One. 2009; 4(2): e4447.
15. Filippov IV, Williams WC, Krebs AA, Pugachev KS. Dynamics of infraslow potentials in the primary auditory cortex: component analysis and contribution of specific thalamic-cortical and non-specific brainstem-cortical influences. Brain Res. 2008; 1219: 66–77.
16. He BJ, Raichle ME. The fMRI signal, slow cortical potential and consciousness. Trends Cogn Sci. 2009; 13(7): 302–309.
17. Logothetis NK, Wandell BA. Interpreting the BOLD signal. Annu Rev Physiol. 2004; 66: 735–769.
18. Pickenhain L, Klingberg F. Hippocampal slow wave activity as a correlate of basic behavioral mechanisms in the rat. Prog Brain Res. 1967; 27: 218–227.
19. Bergmann BM, Winter JB, Rosenberg RS, Rechtschaffen A. NREM sleep with low-voltage EEG in the rat. Sleep. 1987; 10(1): 1–11.
20. Jarosiewicz B, McNaughton BL, Skaggs WE. Hippocampal population activity during the small-amplitude irregular activity state in the rat. J Neurosci. 2002; 22(4): 1373–1384.
21. Vanderwolf CH. Limbic-diencephalic mechanisms of voluntary movement. Psychol Rev. 1971; 78(2): 83–113.
22. Miyawaki H, Diba K. Regulation of Hippocampal Firing by Network Oscillations during Sleep. Curr Biol. 2016; 26(7): 893–902.
23. Schomburg EW, Fernández-Ruiz A, Mizuseki K, et al. Theta phase segregation of input-specific gamma patterns in entorhinal-hippocampal networks. Neuron. 2014; 84(2): 470–485.
24. Watson BO, Levenstein D, Greene JP, Gelinas JN, Buzsáki G. Network homeostasis and state dynamics of neocortical sleep. Neuron. 2016; 90(4): 839–852.
25. Diba K, Buzsáki G. Hippocampal network dynamics constrain the time lag between pyramidal cells across modified environments. J Neurosci. 2008; 28(50): 13448–13456.
26. Csicsvari J, Hirase H, Czurko A, Buzsáki G. Reliability and state dependence of pyramidal cell-interneuron synapses in the hippocampus: an ensemble approach in the behaving rat. Neuron. 1998; 21(1): 179–189.
27. Sirota A, Montgomery S, Fujisawa S, Isomura Y, Zugaro M, Buzsáki G. Entrainment of neocortical neurons and gamma oscillations by the hippocampal theta rhythm. Neuron. 2008; 60(4): 683–697.
28. Barthó P, Hirase H, Monconduit L, Zugaro M, Harris KD, Buzsáki G. Characterization of neocortical principal cells and interneurons by network interactions and extracellular features. J Neurophysiol. 2004; 92(1): 600–608.
29. Schmitzer-Torbert N, Jackson J, Henze D, Harris K, Redish AD. Quantitative measures of cluster quality for use in extracellular recordings. Neuroscience. 2005; 131(1): 1–11.
30. Hazan L, Zugaro M, Buzsáki G. Klusters, NeuroScope, NDManager: a free software suite for neurophysiological data processing and visualization. J Neurosci Methods. 2006; 155(2): 207–216.
31. Bokil H, Andrews P, Kulkarni JE, Mehta S, Mitra PP. Chronux: a platform for analyzing neural signals. J Neurosci Methods. 2010; 192(1): 146–151.
32. Robinson TE, Kramis RC, Vanderwolf CH. Two types of cerebral activation during active sleep: relations to behavior. Brain Res. 1977; 124(3): 544–549.
33. Buzsáki G. Theta oscillations in the hippocampus. Neuron. 2002; 33(3): 325–340.
34. Diba K, Amarasingham A, Mizuseki K, Buzsáki G. Millisecond timescale synchrony among hippocampal neurons. J Neurosci. 2014; 34(45): 14984–14994.
35. Sullivan D, Mizuseki K, Sorgi A, Buzsáki G. Comparison of sleep spindles and theta oscillations in the hippocampus. J Neurosci. 2014; 34(2): 662–674.
36. Isomura Y, Sirota A, Ozen S, et al. Integration and segregation of activity in entorhinal-hippocampal subregions by neocortical slow oscillations. Neuron. 2006; 52(5): 871–882.
37. Hahn TT, Sakmann B, Mehta MR. Phase-locking of hippocampal interneurons' membrane potential to neocortical up-down states. Nat Neurosci. 2006; 9(11): 1359–1361.
38. Hahn TT, McFarland JM, Berberich S, Sakmann B, Mehta MR. Spontaneous persistent activity in entorhinal cortex modulates cortico-hippocampal interaction in vivo. Nat Neurosci. 2012; 15(11): 1531–1538.
39. Grosmark AD, Mizuseki K, Pastalkova E, Diba K, Buzsáki G. REM sleep reorganizes hippocampal excitability. Neuron. 2012; 75(6): 1001–1007.
40. Johnson LA, Euston DR, Tatsuno M, McNaughton BL. Stored-trace reactivation in rat prefrontal cortex is correlated with down-to-up state fluctuation density. J Neurosci. 2010; 30(7): 2650–2661.
41. Luczak A, Barthó P, Marguet SL, Buzsáki G, Harris KD. Sequential structure of neocortical spontaneous activity in vivo. Proc Natl Acad Sci U S A. 2007; 104(1): 347–352.
42. Ji D, Wilson MA. Coordinated memory replay in the visual cortex and hippocampus during sleep. Nat Neurosci. 2007; 10(1): 100–107.
43. Billeh YN, Schaub MT, Anastassiou CA, Barahona M, Koch C. Revealing cell assemblies at multiple levels of granularity. J Neurosci Methods. 2014; 236: 92–106.
44. Jarosiewicz B, Skaggs WE. Hippocampal place cells are not controlled by visual input during the small irregular activity state in the rat. J Neurosci. 2004; 24(21): 5070–5077.
45. Kay K, Sosa M, Chung JE, Karlsson MP, Larkin MC, Frank LM. A hippocampal network for spatial coding during immobility and sleep. Nature. 2016; 531(7593): 185–190.
46. Massimini M, Huber R, Ferrarelli F, Hill S, Tononi G. The sleep slow oscillation as a traveling wave. J Neurosci. 2004; 24(31): 6862–6870.

47. Achermann P, Dijk DJ, Brunner DP, Borbély AA. A model of human sleep homeostasis based on EEG slow-wave activity: quantitative comparison of data and simulations. Brain Res Bull. 1993; 31(1-2): 97–113.
48. Hulse BK, Lubenov EV, Siapas AG. Brain State Dependence of Hippocampal Subthreshold Activity in Awake Mice. Cell Rep. 2017; 18(1): 136–147.
49. Halász P, Terzano M, Parrino L, Bódizs R. The nature of arousal in sleep. J Sleep Res. 2004; 13(1): 1–23.
50. Jarosiewicz B, Skaggs WE. Level of arousal during the small irregular activity state in the rat hippocampal EEG. J Neurophysiol. 2004; 91(6): 2649–2657.
51. Roldan E, Weiss T, Fifkova E. Excitability changes during the sleep cycle of the rat. Electroencephalogr Clin Neurophysiol. 1963; 15: 775–785.
52. Terzano MG, Mancia D, Salati MR, Costani G, Decembrino A, Parrino L. The cyclic alternating pattern as a physiologic component of normal NREM sleep. Sleep. 1985; 8(2): 137–145.
53. Girardeau G, Cei A, Zugaro M. Learning-induced plasticity regulates hippocampal sharp wave-ripple drive. J Neurosci. 2014; 34(15): 5176–5183.
54. Penttonen M, Nurminen N, Miettinen R, et al. Ultra-slow oscillation (0.025 Hz) triggers hippocampal afterdischarges in Wistar rats. Neuroscience. 1999; 94(3): 735–743.
55. Vanhatalo S, Palva JM, Holmes MD, Miller JW, Voipio J, Kaila K. Infraslow oscillations modulate excitability and interictal epileptic activity in the human cortex during sleep. Proc Natl Acad Sci USA. 2004; 101(14): 5053–5057.
56. Compte A, Sanchez-Vives MV, McCormick DA, Wang XJ. Cellular and network mechanisms of slow oscillatory activity (<1 Hz) and wave propagations in a cortical network model. J Neurophysiol. 2003; 89(5): 2707–2725.
57. Kudrimoti HS, Barnes CA, McNaughton BL. Reactivation of hippocampal cell assemblies: effects of behavioral state, experience, and EEG dynamics. J Neurosci. 1999; 19(10): 4090–4101.
58. Genzel L, Kroes MC, Dresler M, Battaglia FP. Light sleep versus slow wave sleep in memory consolidation: a question of global versus local processes? Trends Neurosci. 2014; 37(1): 10–19.
59. Halász P. Hierarchy of micro-arousals and the microstructure of sleep. Neurophysiol Clin. 1998; 28(6): 461–475.
60. Kuga N, Sasaki T, Takahara Y, Matsuki N, Ikegaya Y. Large-scale calcium waves traveling through astrocytic networks in vivo. J Neurosci. 2011; 31(7): 2607–2614.
61. Chen Y, Swanson RA. Astrocytes and brain injury. J Cereb Blood Flow Metab. 2003; 23(2): 137–149.
62. Porkka-Heiskanen T, Kalinchuk AV. Adenosine, energy metabolism and sleep homeostasis. Sleep Med Rev. 2011; 15(2): 123–135.
63. Halassa MM, Florian C, Fellin T, et al. Astrocytic modulation of sleep homeostasis and cognitive consequences of sleep loss. Neuron. 2009; 61(2): 213–219.

SUPPLEMENTARY MATERIAL

Supplementary material is available at *SLEEP* online https://doi.org/10.1093/sleep/zsx066.

FUNDING

This work was partially supported by National Institutes of Health [grant no. R01MH109170].

ACKNOWLEDGMENTS

We are grateful to Adrien Peyrache, Kenji Mizuseki, and crcns.org for making their data readily available, and Christof Koch, Markus Schmidt, and Brendon O. Watson for valuable comments.

SUBMISSION & CORRESPONDENCE INFORMATION

Submitted for publication November, 2016
Submitted in final revised form March, 2017
Accepted for publication April, 2017
Address correspondence to: Kamran Diba, PhD, Department of Psychology, Box 413, University of Wisconsin—Milwaukee, Milwaukee, WI 53201, USA. Telephone: 414-229-5740; Fax: 414-229-5219; Email: diba@uwm.edu

AUTHORS' NOTE

HM performed research. YNB performed analyses identifying LOW-active cells. HM and KD designed research and wrote the manuscript, with comments from YNB.

DISCLOSURE STATEMENT

None declared. A previous version of this paper was published in BioRXiv. This work was performed at the University of Wisconsin—Milwaukee.